

**Full Paper**

**Montmorillonite/carboxymethylcellulose-composite hydrogel beads as biodegradable adsorbent for dye removal**

**Pranee Rojsitthisak<sup>1,\*</sup>, Supakarn Hansapaiboon<sup>2</sup>, Feuangthit Niyamissara Sorasitthiyanukarn<sup>1</sup> and Sarinthorn Limpanart<sup>1</sup>**

<sup>1</sup> Metallurgy and Materials Science Research Institute, Chulalongkorn University, Bangkok 10330, Thailand

<sup>2</sup> Pharmaceutical Research Instrument Center, Faculty of Pharmaceutical Sciences, Chulalongkorn University, Bangkok 10330, Thailand

\* Corresponding author, e-mail: [pranee.l@chula.ac.th](mailto:pranee.l@chula.ac.th)

*Received: 6 March 2018 / Accepted: 23 August 2019 / Published: 2 September 2019*

---

**Abstract:** Montmorillonite/carboxymethylcellulose (MMT/CMC)-composite hydrogel beads with different MMT/CMC mass ratios were prepared by coacervation using iron (III) chloride as crosslinking agent. The effects of MMT/CMC mass ratio, pH of cationic dye solution, initial dye concentration and diameter of beads on the adsorption capacity of MMT/CMC-composite beads compared with CMC beads were examined. The inclusion of MMT increases the adsorption capacity of CMC beads in a dose-dependent manner, reaching an adsorption capacity of 13 mg dye/g beads when the beads contain the MMT/CMC mass ratio of 0.4:1 and the cationic dye solution pH is between 7-9. In addition, a smaller diameter of the beads gives a better dye adsorption capacity. Finally, the adsorption process can be described by the Langmuir isotherm model. The MMT/CMC-composite beads can potentially be used as an ecofriendly or green adsorbent to remove cationic dyes from industrial wastewater.

**Keywords:** carboxymethylcellulose, cationic dye adsorption, hydrogel beads, montmorillonite

---

## INTRODUCTION

Water pollution has become a major global problem following the rapid industrial development including industries that use dyes to colour their products, such as textile, paper and plastic industries. In the world market, over  $7 \times 10^5$  metric tons of dyestuffs are produced annually [1] and most of these are hazardous and toxic, causing allergic and carcinogenic effects to humans [2]. Therefore, dye removal from industrial wastewater before discharge to the environment is very important for environmental management systems [3].

Nowadays, several technologies have been applied for dye removal, such as membrane filtration [4,5], oxidation [6], flocculation [5], ion-exchange [7] and adsorption [1,8,9]. Among these technologies, adsorption is considered as a powerful technique for dye removal. For example, activated carbon is conventionally used for removal of dyes and organic pollutants from industrial wastewater due to its microporous structure, large surface area and high adsorption capacity [1]. However, it is quite expensive and has a high regeneration cost [10]. In addition, its amount and uptake capacity are reduced by 10-15% after regeneration by the refractory technique [11]. Therefore, there is a search for alternative low-cost materials that are effective and biodegradable, such as agricultural wastes [1], hydrogel beads [12] and montmorillonite (MMT) [13,14].

In the case of agricultural wastes such as corn peel, rice husk, orange peel, banana peel, oil palm trunk fibre and durian peel [1], they mainly contain cellulose, which is quite compact and inactive [15]. To make cellulose more hydrophilic and amorphous, which are requirements for adsorbents [16], their structures need to be modified, e.g. by carboxymethylation [15] to produce carboxymethylcellulose (CMC).

As a water-soluble cellulose derivative, CMC is widely used as an adsorbent for dye removal from wastewaters [15,17]. To improve its adsorption ability, CMC should be in the form of three-dimensional networks or hydrogels [18], which are hydrophilic network structures, and should contain several functional groups that can adsorb the dyes or metal ions from the wastewater [19-22]. However, most conventional hydrogels are derived from synthetic polymers that are not biodegradable and have a high production cost and low stability [23]. To overcome these restrictions, naturally occurring polymers, which are mainly polysaccharides, have been used for the preparation of hydrogels, where their adsorption capacity is enhanced by addition of clay-minerals [8,9].

The clay mineral MMT is considered an excellent adsorbent of proteins and heavy metals because of its chemical nature, pore structure, high cationic exchange efficiency and chemical stability [24,25]. In addition, MMT is non-toxic and inexpensive, but its adsorption ability is limited by its poor water permeability. To overcome this limitation, MMT has been blended with other materials to make composites with high water permeability, and these composites have been used as adsorbents for wastewater treatment [26-28]. However, the use of MMT/CMC-composite hydrogel beads as adsorbent for cationic dye removal has not been studied. Therefore, this study was undertaken to examine the adsorption capacity of MMT/CMC-composite hydrogel beads for Maxilon Red GRL cationic dye by varying the MMT/CMC mass ratio, pH of dye solution, initial dye concentration and diameter of the composite hydrogel beads. To describe the adsorption character, adsorption isotherm models were investigated.

## **MATERIALS AND METHODS**

### **Materials**

Sodium-MMT with a zeta potential of -39.3 mV and a cationic exchange capacity of 71 mequiv/100 g was purchased from Southern Clay (USA) while the cationic dye (Maxilon Red GRL 200%) was supplied by Ciba Specialty Chemicals (Thailand). Anhydrous iron (III) chloride (sublimed) was supplied by Carlo Erba Reagents (France). CMC (molecular weight 580,000 g/mol; degree of substitution 0.8) was prepared from bleached cellulose fibre by etherification with monochloroacetic acid, as described by Rojsitthisak et al. [29] with modification. Briefly, bleached cellulose fibre from corn peel collected from Chulalongkorn University canteen was prepared by

soaking the dried peel in 3% (w/v) NaOH solution (liquid/material ratio = 20:1 (v:w)) at 90°C for 2 hr, followed by treatment with 0.7% (w/v) hydrogen peroxide solution (liquid/material ratio = 15:1 (v:w)) under alkaline condition at 90°C for 90 min. The bleached cellulose fibre (5 g) was then suspended in 95% (v/v) ethanol : 45% (w/v) NaOH (10:1 (v/v)) (110 mL) at 60°C for 60 min. before addition of monochloroacetic acid (5 g) to the suspension, left at room temperature for 6 hr and then incubated at 70°C for 60 min. The obtained CMC was neutralised with glacial acetic acid, purified by Soxhlet extraction using ethanol and dried at 80°C. The degree of substitution of CMC was analysed based on ASTM D 1439-03 and its molecular weight was determined by gel permeation chromatography using pullulan as a polymer standard.

A 4% (w/v) CMC stock solution was prepared by dissolving 4 g of CMC in 100 mL of deionised water with vigorous stirring for 1 hr. Iron (III) chloride (5.5% (w/v)) and cationic dye (60 mg/L) solutions were prepared in deionised water.

### Preparation of MMT/CMC-Composite Hydrogel Beads

The MMT/CMC suspensions with different mass ratios (0.0:1, 0.1:1, 0.2:1 and 0.4:1) were prepared by adding sodium-MMT to the 4% (w/v) CMC stock solution at 0, 0.4, 0.8 and 1.6% (w/v) respectively under vigorous dispersion for 1 hr. The MMT/CMC suspension (100 mL) was then added dropwise to 5.5% (w/v) iron (III) chloride solution (500 mL) using a peristaltic pump at 25, 26, 27 and 29 mL/hr for the MMT/CMC ratios of 0.0:1, 0.1:1, 0.2:1 and 0.4:1 respectively. After slowly stirring for 1 hr, the solidified MMT/CMC-composite hydrogel beads were harvested by filtration and washed with deionised water several times until free from chloride and then dried at 60°C for 24 hr.

### Adsorption Experiments

All batch adsorption experiments were performed on a shaker (150 rpm) at room temperature. The effect of contact time on the adsorption was performed using 0.2 g MMT/CMC-composite hydrogel beads, formed from the different MMT/CMC mass ratios, and 50 mL of cationic dye solution (60 mg/L) in a 125-mL conical flask. The dye solution was collected at intervals over 11 days and the residual dye concentration was measured using a UV-vis spectrophotometer (model Specord S 100, Analytik Jena AG, Germany) at 287 nm. The amount of adsorbed dye at time  $t$  was calculated from Eq. 1:

$$Q_t = (C_0 - C_t)V/W, \quad (1)$$

where  $Q_t$  is amount of adsorbed dye per amount of beads at time  $t$  (mg/g),  $C_0$  is initial concentration of cationic dye in solution (mg/L),  $C_t$  is concentration of cationic dye in solution at time  $t$  (mg/L),  $W$  is weight of dried composite hydrogel beads (g) and  $V$  is volume of dye solution (L).

To study effects of pH, initial concentration of cationic dye solution and diameter of beads, the experiment was performed as described above except that the contact time was fixed at the deduced equilibrium point. The equilibrium adsorption capacity ( $Q_e$ ) of the composite hydrogel beads was calculated from Eq. 2:

$$Q_e = (C_0 - C_e)V/W, \quad (2)$$

where  $C_0$  and  $C_e$  are initial concentration and equilibrium concentration of cationic dye in solution (mg/L) respectively,  $V$  is volume of dye solution (L) and  $W$  is weight of dried composite hydrogel beads (g).

## Characterisation of MMT/CMC Hydrogel Beads and Their Precursors

The MMT, CMC powder, CMC hydrogel beads and MMT/CMC-composite hydrogel beads were characterised by Fourier transform infrared (FTIR) spectrophotometry (model Spectrum 400, Perkin Elmer, Spectrum One, USA) using KBr disc. The measurement was performed using a transmittance mode from 4,000 to 400  $\text{cm}^{-1}$  with 16 scans per sample at a resolution of 4  $\text{cm}^{-1}$ . The crystallinity of the samples was determined by wide-angle X-ray diffraction (XRD; model PW3710, Philips, Netherlands). The analysis was performed at 40 kV and 30 mA using Cu  $K_{\alpha}$  radiation (1.54 Å) and scanning speed of 0.2° (2 $\Theta$ )/step at room temperature. The anhydrous morphology of the composite hydrogel beads was visualised by scanning electron microscopy (SEM; model Quanta 250, FEI, Netherlands). Thermal properties of the composite beads were determined by thermogravimetric analysis (TGA; model TGA/SDTA851<sup>e</sup>, Mettler Toledo, Switzerland) under nitrogen gas flow from 30°C to 800°C at a heating rate of 10°C/min. Differential scanning calorimetry analysis (DSC; model DSC 204F1 Phoenix<sup>®</sup>, Germany) was performed under nitrogen gas flow from 25°C to 300°C at a heating rate of 5°C/min. The swelling of the beads was calculated from weight difference of beads before and after dye adsorption as percentage of initial weight of the dried beads.

### Statistical Analysis

All experiments were performed in triplicate and the data are presented as mean  $\pm$  standard deviation (SD). Statistical analysis was performed by one-way ANOVA using Microsoft Excel and accepting statistical significance at  $p < 0.05$  level.

## RESULTS AND DISCUSSION

### Characteristics of MMT/CMC-Composite Hydrogel Beads

#### *Characterisation by FTIR analysis*

Representative FTIR spectra of the MMT powder, MMT/CMC-composite hydrogel beads, CMC hydrogel beads and CMC powder are shown in Figure 1, where the circle indicates the functional groups of Si-O and Al-O of MMT powder in the MMT/CMC-composite hydrogel beads (with MMT/CMC mass ratio of 0.4:1 as representative example). The characteristic peaks of CMC at 1600  $\text{cm}^{-1}$  (asymmetric stretching of COO<sup>-</sup>) and 1420  $\text{cm}^{-1}$  (symmetric stretching of COO<sup>-</sup>) are observed in the MMT/CMC-composite hydrogel beads. In addition, the MMT/CMC-composite and CMC hydrogel beads both show an extra peak at 1750  $\text{cm}^{-1}$ , which is absent in the CMC powder. This peak indicates the electrostatic interaction between the C=O of CMC and iron (III). Swamy and Yun [30] found a small peak at 1751  $\text{cm}^{-1}$  in sodium alginate-sodium CMC hydrogel beads, which may have been caused by the electrostatic interaction between the carboxylic groups of alginate and CMC with iron (III). These results provide evidence of crosslinking between the polymer composite and iron (III).

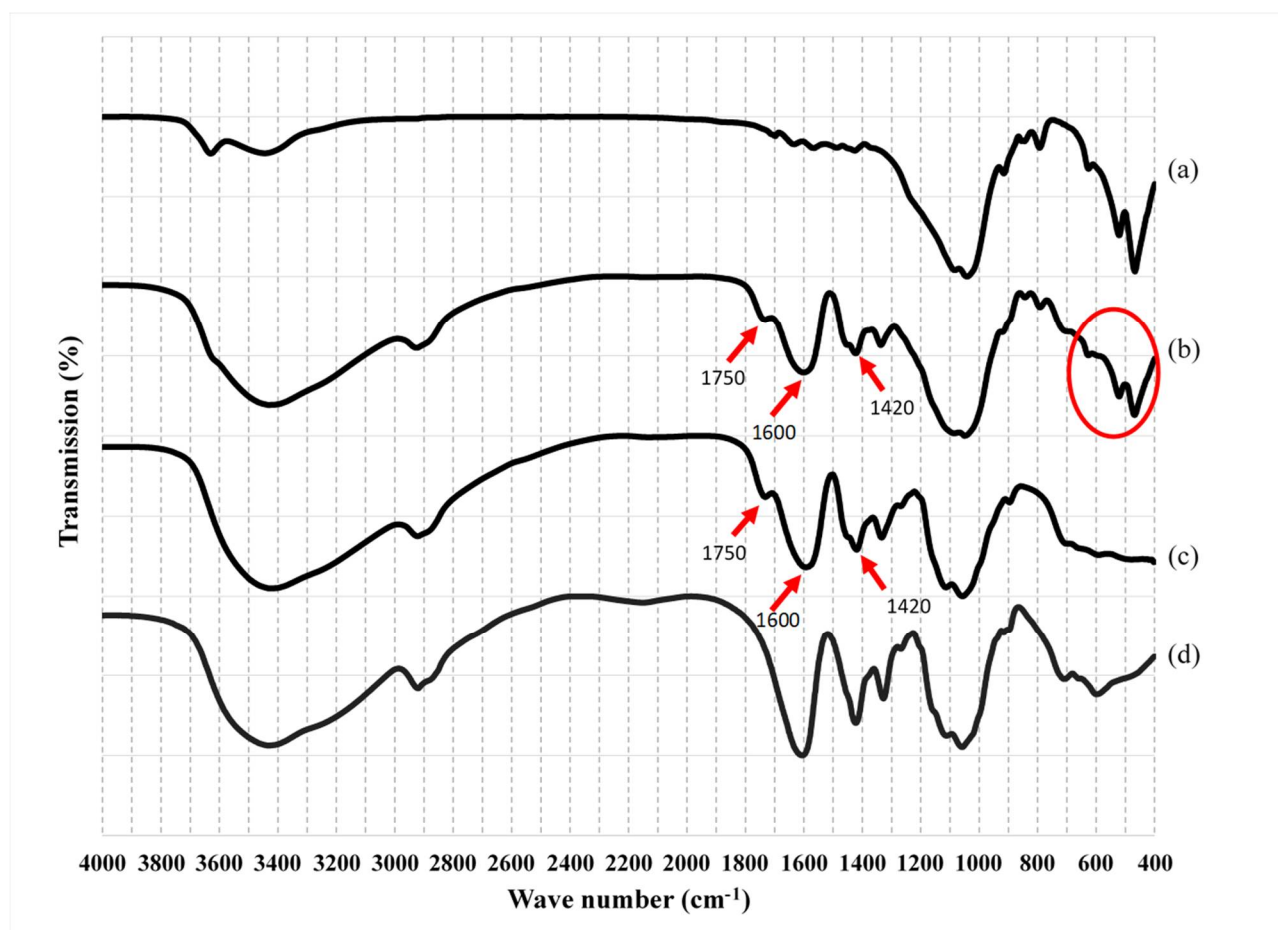


**Figure 1.** Representative FTIR spectra of (a) MMT powder, (b) MMT/CMC-composite hydrogel beads (MMT/CMC = 0.4:1 (w/w)), (c) CMC hydrogel beads and (d) CMC powder

### *XRD analysis*

Representative XRD diffractograms of the MMT powder, MMT/CMC-composite hydrogel beads (with MMT/CMC mass ratio of 0.4:1 as representative example) and CMC hydrogel beads are presented in Figure 2. The sharp characteristic diffraction peak of MMT in the 001 plane at  $6.01^{\circ}2\theta$  is observed, whereas this peak is not present in the diffractogram of the MMT/CMC-composite hydrogel beads or the CMC hydrogel beads. This suggests that the CMC molecules had penetrated into the layers of MMT and an exfoliated structure had formed [26]. In addition, the peaks located at wave numbers between  $400\text{--}600\text{ cm}^{-1}$  in the FTIR spectrum of the MMT/CMC-composite hydrogel beads (Figure 1) confirm that MMT was incorporated into the MMT/CMC-composite hydrogel beads. Therefore, the XRD diffractogram of the MMT/CMC-composite hydrogel beads represents an exfoliated MMT in the MMT/CMC-composite hydrogel beads.

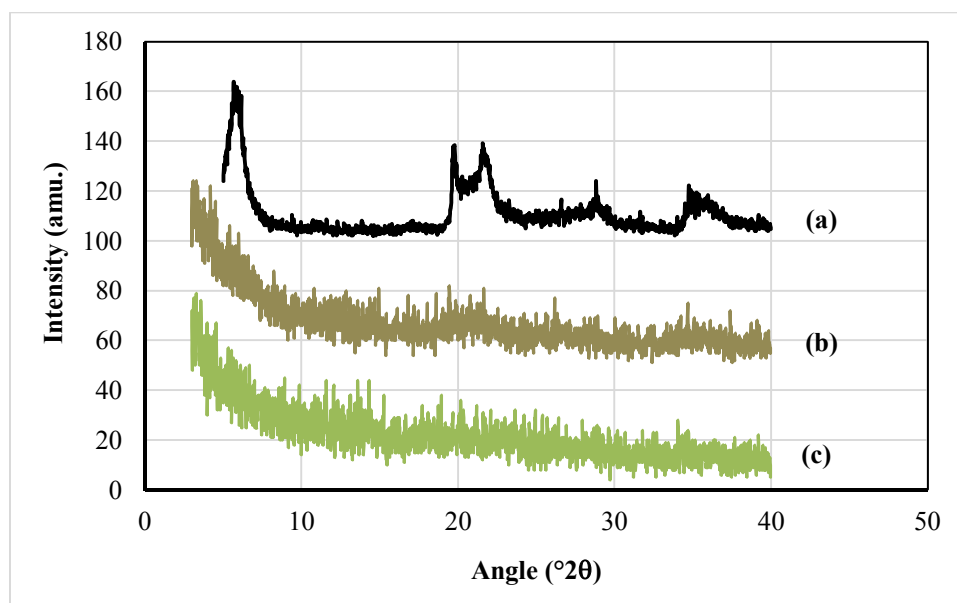


**Figure 2.** Representative XRD of (a) MMT powder, (b) MMT/CMC-composite hydrogel beads (MMT/CMC = 0.4:1 (w/w)) and (c) CMC hydrogel beads

### *Thermal property*

The TGA thermogram of the MMT/CMC-composite hydrogel beads, compared with those of the MMT powder and CMC hydrogel beads, is shown in Figure 3A. At 25°C to 200°C, the percentage weight loss of the CMC hydrogel beads is higher than that of the MMT/CMC-composite hydrogel beads, which indicates a better thermal stability of the MMT/CMC-composite hydrogel beads than that of the CMC hydrogel beads. At 800°C the percentage weight residue of the MMT/CMC-composite hydrogel beads (45.3%) is larger than that of the CMC hydrogel beads (27.6%) by about 17.7%, which is taken to indicate the amount of MMT in the MMT/CMC-composite.

The thermal behaviour of the MMT/CMC-composite hydrogel beads (with an MMT/CMC mass ratio of 0.4:1 as representative example) and CMC hydrogel beads, as evaluated by DSC analysis, is shown in Figure 3B. The endothermic peak of the CMC hydrogel beads starts at 182.2°C and shows a maximum peak at 192.2°C, which indicates the pyrolysis of CMC. On the other hand, the pyrolysis of CMC in MMT/CMC-composite hydrogel beads is shifted up to 189.2°C and there are two nodes of maximum peaks. This indicates that an interaction between MMT and CMC occurs and the crystal structure of CMC in MMT/CMC-composite hydrogel beads is changed. Consequently, more energy is required for the decomposition of CMC molecules in the MMT/CMC-composite hydrogel beads.

### *SEM analysis*

The morphology of the CMC hydrogel beads and MMT/CMC-composite hydrogel beads with different MMT/CMC mass ratios, as visualised by SEM, is shown in Figure 4. The surface roughness of the CMC hydrogel beads occurs when the CMC chains contract rapidly with cohesion force during the drying process (Figure 4(a)). However, the surface of the CMC hydrogel beads is quite smooth compared to that of the MMT/CMC-composite hydrogel beads (Figure 4(b)-(d)). This

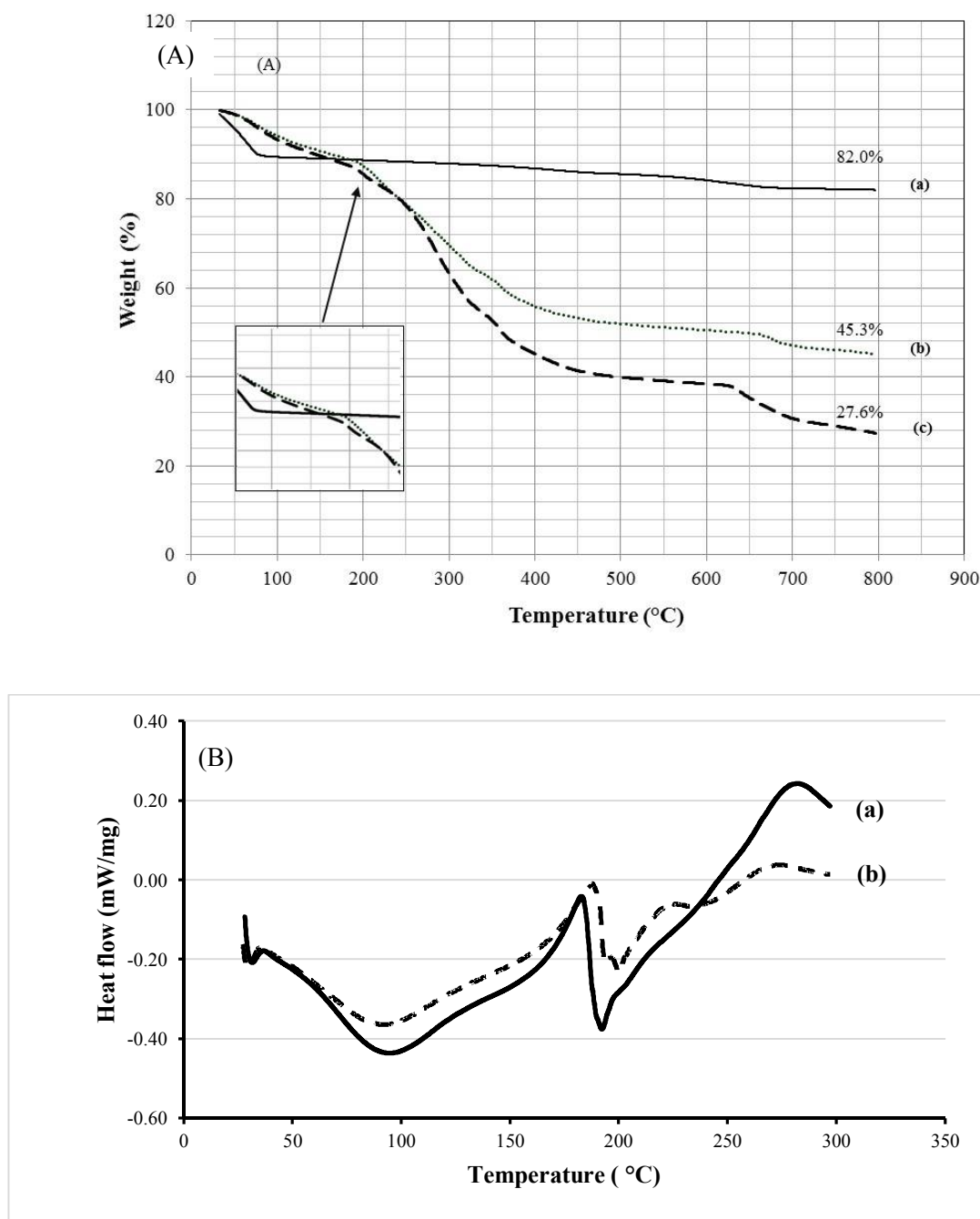


**Figure 3.** Representative TGA (A) and DSC (B) thermograms of (a) MMT powder, (b) MMT/CMC-composite hydrogel beads (MMT/CMC = 0.4:1 (w/w)) and (c) CMC hydrogel beads

can be explained by the fact that the contraction of the CMC chains during drying might have been interrupted by movement of the MMT particles, resulting in an increases roughness of the beads [31]. In addition, this surface roughness increases with increasing levels of MMT in the MMT/CMC-composite hydrogel beads. This suggests that the MMT/CMC-composite hydrogel beads have a higher surface area than the CMC beads and consequently a higher contact area, a potentially desirable property for dye adsorption.



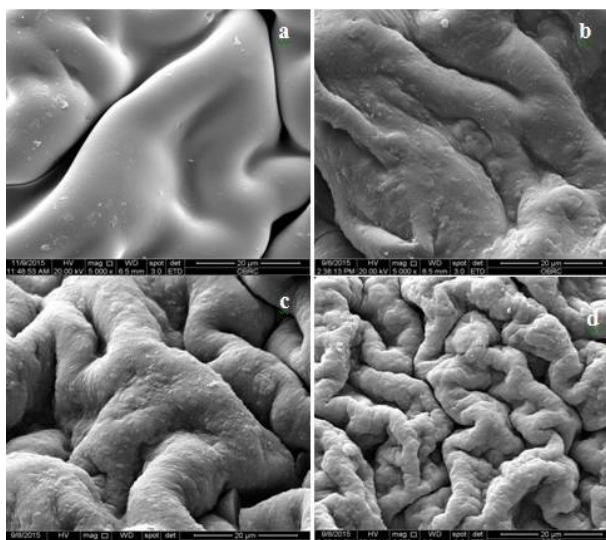


**Figure 4.** Representative SEM images of the MMT/CMC-composite hydrogel beads at MMT/CMC mass ratios of (a) 0.0:1 (CMC beads), (b) 0.1:1, (c) 0.2:1 and (d) 0.4:1 (magnification: x 5,000)

#### Effect of Adsorbent-Adsorbate Contact Time

Figure 5 shows the amounts of the cationic dye that are adsorbed onto the CMC hydrogel beads and MMT/CMC-composite hydrogel beads at different contact times. Increasing the contact time results in an increased amount of cationic dye adsorbed on both the CMC hydrogel beads and MMT/CMC-composite hydrogel beads, but with different equilibrium times and maximum adsorption capacities between them. For example, the CMC hydrogel beads reached equilibrium at 4 days with a maximum adsorption capacity of 3.3 mg/g beads, whereas the MMT/CMC-composite hydrogel beads with MMT/CMC mass ratios of 0.1:1, 0.2:1 and 0.4:1 reach equilibrium at 7, 9 and 11 days respectively, with maximum adsorption capacities of 7.3, 8.5 and 13 mg/g beads respectively. A larger amount of MMT in the MMT/CMC-composite could result in a higher negative charge density on the surface of the MMT/CMC hydrogel beads, so they can adsorb more cationic dye on their surface. Wang and Wang [26] also reported similar results and suggested that the cationic dye might be adsorbed on the negative charges of MMT present on the surface of the composite beads via electrostatic attraction. To make sure that all types of MMT/CMC-composite hydrogel beads in this study have reached equilibrium for cationic dye adsorption, a contact time of 11 days is selected for further study.

In addition, the swelling of the hydrogel beads after equilibrium (day 11) also depends on the amount of MMT in the MMT/CMC-composite, as shown in Table 1. The swelling of the composite hydrogel beads with MMT/CMC mass ratios of 0.1:1, 0.2:1 and 0.4:1 is significantly higher than that of the CMC beads (MMT/CMC ratio = 0.0:1) by about 11%, 16% and 24% respectively. The increased MMT proportion might result in a higher negative charge density that interacts with water. Furthermore, the rougher surface and higher surface area of the composite hydrogel beads (Figure 4) likely enhances their ability to adsorb the dye.



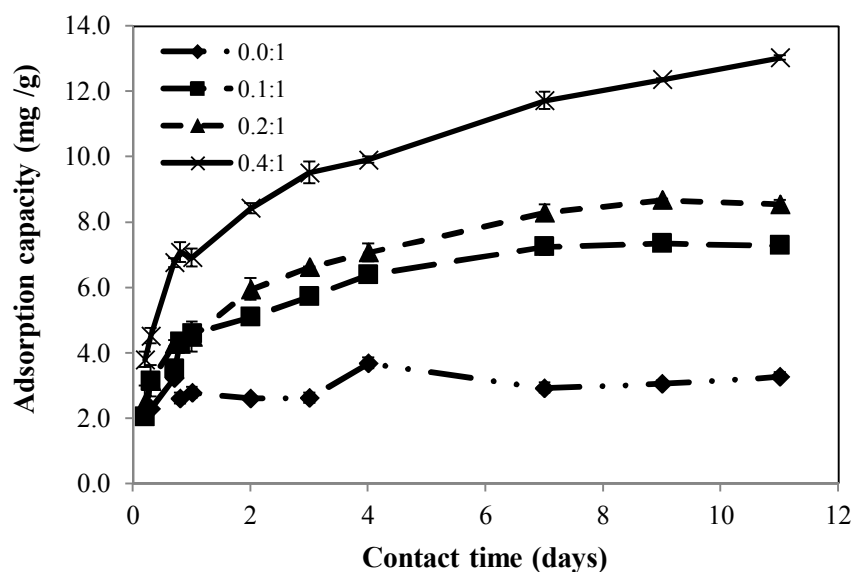


**Figure 5.** Effect of contact time on cationic dye adsorption capacity of MMT/CMC-composite hydrogel beads with different MMT/CMC mass ratios (initial dye concentration = 60 mg/L, without adjusted pH). Data are shown as mean  $\pm$  SD of 3 independent trials.

**Table 1.** Swelling of MMT/CMC-composite hydrogel beads containing different MMT/CMC mass ratios after equilibrium (no pH adjustment)

MMT/CMC mass ratio	Swelling (%)
0.0:1	22.7 $\pm$ 0.3
0.1:1	25.2 $\pm$ 0.7
0.2:1	26.3 $\pm$ 0.5
0.4:1	28.1 $\pm$ 1.5

Note: Data are shown as mean  $\pm$  SD of 3 independent trials.

### Effect of pH of Dye Solution

The initial pH of the dye solution is one of the crucial parameters that affect the adsorption of charged (ionic) dyes. The adsorption capacity of all the hydrogel beads after equilibrium (11 days) is minimal at pH 3.0 and gradually increases with increasing pH up to pH 7.0, and then remains almost constant to pH 9 (Figure 6). This phenomenon can be explained by the fact that  $H^+$  ions in acidic conditions ( $pH < 7$ ) compete with the positively charged cationic dye to adsorb onto the hydrogel beads, resulting in a lower cationic dye adsorption on the anionic surface of the hydrogel beads [1]. On the other hand, increasing the pH (3–9) leads to the surface of the hydrogel beads, especially those of the MMT/CMC-composite, becoming ionised with a higher anionic surface charge density to electrostatically interact more with the cationic dye.

Comparison of the CMC hydrogel beads (MMT/CMC ratio = 0.0:1) with MMT/CMC hydrogel beads reveals that the dye adsorption capacity of the beads increases with increasing proportion of MMT at all pH values between pH 3–9, although this is less marked between beads with MMT/CMC ratios of 0.1:1 and 0.2:1. For example, at pH 7 the adsorption capacity of the hydrogel beads with MMT/CMC ratio of 0.4:1 is 12.0 mg/g, whereas for those with MMT/CMC ratios of 0.0:1, 0.1:1 and 0.2:1, the adsorption values are 4.98, 7.44 and 7.73 mg/g respectively.

The pH of the dye solution does not significantly affect the swelling behaviour of the beads over the tested range (pH 3-9, data not shown). However, the percentage of swelling increases with increasing MMT proportions, where the average swelling of MMT/CMC beads with a MMT/CMC mass ratio of 0:0, 0.1:1, 0.2:1 and 0.4:1 (calculated from pH 3-9) is 19.6%, 20.7%, 20.6% and 23.0% respectively. Thus, the pH of dye solution was set at pH 7 and the composite hydrogel with a MMT/CMC ratio of 0.4:1 was chosen for further studies in comparison with the CMC hydrogel.

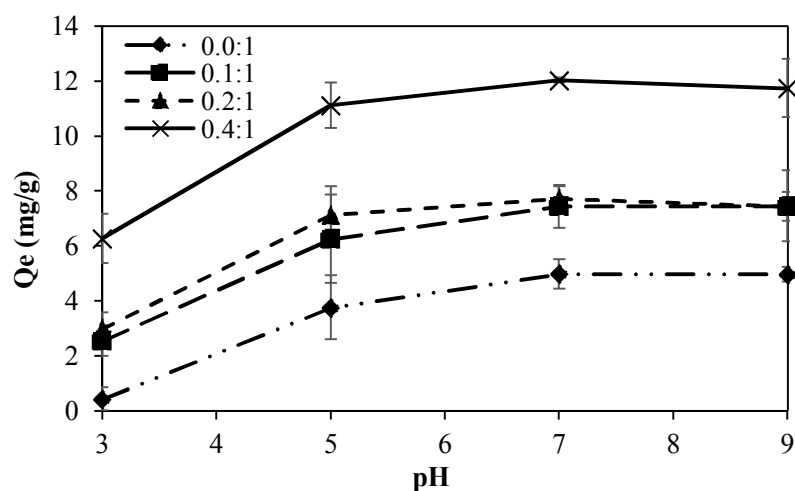


**Figure 6.** Effect of dye solution pH on dye adsorption capacity of MMT/CMC-composite hydrogel beads with different MMT/CMC mass ratios (initial dye concentration = 60 mg/L, contact time = 11 days). Data are shown as mean  $\pm$  SD of 3 independent trials.

### Effect of Bead Diameter

The effect of different bead diameters on their adsorption capacity for the cationic dye is summarised in Table 2. The dye adsorption capacity of both the CMC and MMT/CMC-composite hydrogel beads increase with decreasing bead diameter. For beads with equal weight, those with a smaller diameter have a larger surface area for dye absorption, thus resulting in a higher adsorption capacity. In addition, at each bead diameter, the MMT/CMC beads have a markedly better adsorption capacity than the CMC beads. For example, at the bead diameter of 1 mm, the dye adsorption capacity of the MMT/CMC beads is 2.4-fold higher than that of the CMC beads. This difference increases with increasing bead size to 5.6-fold higher at 2.0-mm diameter.

**Table 2.** Effect of hydrogel bead diameter on its adsorption capacity

Bead diameter (mm)	Adsorption capacity (mg/g)	
	MMT/CMC = 0.0:1	MMT/CMC = 0.4:1
1.0	4.98 $\pm$ 0.53	12.04 $\pm$ 0.10
1.5	2.32 $\pm$ 0.03	10.30 $\pm$ 0.23
2.0	1.95 $\pm$ 0.29	10.87 $\pm$ 0.25

Note: Data are shown as mean  $\pm$  SD of 3 independent trials.

### Effect of Initial Dye Concentration

Increasing the initial dye concentration leads to an increased adsorption capacity in both the CMC and MMT/CMC beads (Figure 7). The maximal amounts of cationic dye adsorbed are 9.05 and 13.44 mg/g respectively. Bulut and Aydin [32] and Begum and Mahbub [33] explain that the driving force for mass transfer is high at high initial dye concentration and consequently a high adsorption capacity is observed. The MMT/CMC beads (MMT/CMC mass ratio of 0.4:1) have the largest dye adsorption capacity so they are chosen for the evaluation of adsorption isotherm.

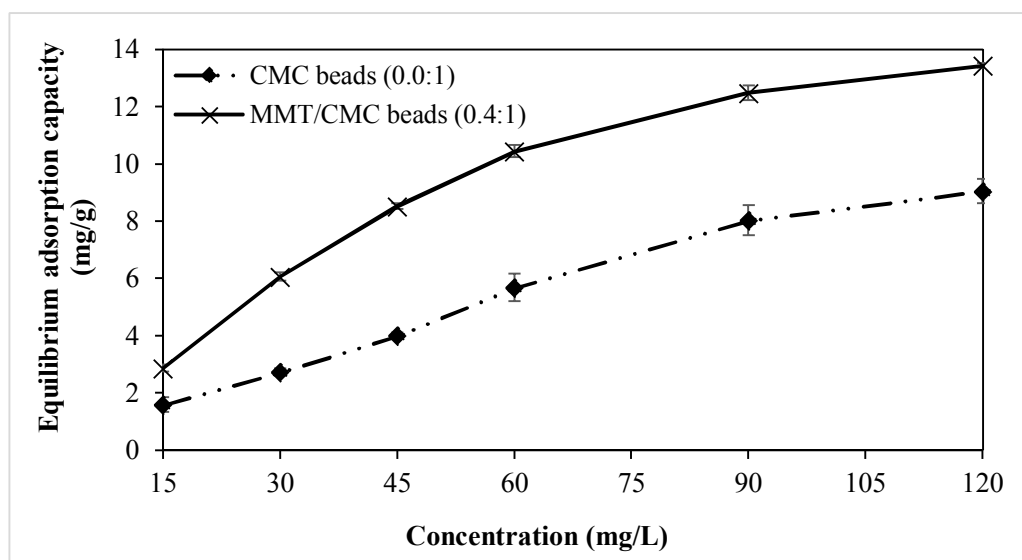


**Figure 7.** Effect of initial dye concentration on adsorption capacity of MMT/CMC-composite hydrogel beads compared with CMC hydrogel beads (pH of dye solution = 7, contact time = 11 days). Data are shown as mean  $\pm$  SD of 3 independent trials.

### Adsorption Isotherm

An adsorption isotherm describes the relationship between the amount of an adsorbate adsorbed on the surface of an adsorbent and the concentration of the dissolved adsorbate in solution at equilibrium. Furthermore, the adsorption isotherm is used for describing the interaction between adsorbate and adsorbent, and also for optimising the use of adsorbent. Among different isotherm models, the Langmuir and the Freundlich isotherms are frequently used to model the adsorption of dyes on polymer surfaces [34-37] so these two models are tested in this study.

The basic assumptions of the Langmuir isotherm model are that adsorption occurs at specific homogeneous sites on the adsorbent and that once the adsorbate occupies a site, no further adsorption can take place at that site [38]. The linear form of the Langmuir equation is expressed in Eq. 3:

$$1/Q_e = 1/Q_{max} + 1/(bQ_{max}C_e), \quad (3)$$

where  $Q_e$  is the adsorption capacity of the adsorbent at equilibrium,  $C_e$  is the dye concentration at equilibrium time,  $b$  is the Langmuir constant and  $Q_{max}$  is the maximum monolayer adsorption capacity. Moreover, a dimensionless constant, commonly known as the separation factor ( $R_L$ ) defined by Weber and Chakravorti [39], can be represented by Eq. 4,

$$R_L = 1/(1+bC_0), \quad (4)$$

Based on the  $R_L$  value, the adsorption process can be categorised as unfavourable ( $R_L > 1$ ), linear ( $R_L = 1$ ), favourable ( $0 < R_L < 1$ ) or irreversible ( $R_L = 0$ ).

On the other hand, the Freundlich isotherm assumes that the adsorbent has an unlimited capacity to adsorb the adsorbate. It suitably describes adsorption onto heterogeneous surfaces and multi-layer adsorption [40]. The linear form of the Freundlich equation, as given by Weber and Chakravorti [39], is shown in Eq. 5:

$$\ln Q_e = \ln K_F + n^{-1} \ln C_e, \quad (5)$$

where  $K_F$  is the Freundlich constant related to the adsorption capacity of the adsorbent and  $n$  is an empirical constant which gives valuable information about the isotherm's shape. Based on the  $n^{-1}$  values, the adsorption process may be classified as irreversible ( $n^{-1} = 0$ ), favourable ( $0 < n^{-1} < 1$ ) or unfavourable ( $n^{-1} > 1$ ).

Based on our experimental results, the linear isotherm coefficients for these models are summarised in Table 3. The values of the dimensionless constant ( $R_L$ ) obtained from the Langmuir model for CMC hydrogel beads and MMT/CMC-composite hydrogel beads are both markedly less than 1, indicating favourable adsorption of the cationic dye onto both samples. For the Freundlich model, the values of the empirical constant ( $n^{-1}$ ) are both likewise below 1, indicating favourable adsorption of the cationic dye onto the two types of hydrogel beads. However, the correlation coefficients ( $R^2$ ) for the Langmuir model are slightly higher than those for the Freundlich model for both the CMC and MMT/CMC beads (Table 3). This implies that the adsorption of the cationic dye onto both types of hydrogel beads follows a Langmuir-type adsorption mechanism with monolayer adsorption occurring at the binding sites on the surface of the beads.

**Table 3.** Langmuir and Freundlich isotherm coefficients for cationic dye adsorption onto CMC hydrogel beads and MMT/CMC-composite hydrogel beads

Adsorbent	Slope	Intercept	$R_L$	$n^{-1}$	$R^2$
<i>Langmuir isotherm model</i>					
CMC hydrogel beads	0.233	17.825	0.034	n/a	0.987
MTT/CMC-composite hydrogel beads	4.393	13.532	0.012	n/a	0.994
<i>Freundlich isotherm model</i>					
CMC hydrogel beads	0.794	-0.484	n/a	0.794	0.984
MTT/CMC-composite hydrogel beads	0.2455	0.722	n/a	0.721	0.956

## CONCLUSIONS

Composite MMT/CMC-hydrogel beads have the potential for being used as biodegradable adsorbent for the removal of a cationic dye from wastewater with neutral to alkaline pH (7-9). The maximum adsorption capacity of the beads is 13 mg/g when they contain MMT/CMC at a mass ratio of 0.4:1. The adsorption process can be described by the Langmuir isotherm model.

## ACKNOWLEDGEMENTS

This research was supported by Ratchadapisaksothomphot Endowment under the Outstanding Research Performance Program, Chulalongkorn University 2015 (GF-58-06-62-01). Special thanks

are due to Dr. Robert D .J. Butcher (Research Clinic Unit of Chulalongkorn University) for his correction of the manuscript.

## REFERENCES

1. K. S. Bharathi and S. T. Ramesh, "Removal of dyes using agricultural waste as low-cost adsorbents: A review", *Appl. Water Sci.*, **2013**, 3, 773-790.
2. D. A. Fungaro, M. Bruno and L. C. Grosche, "Adsorption and kinetic studies of methylene blue on zolite synthesized from fly ash", *Desal. Water Treat.*, **2009**, 2, 231-239.
3. X. Luo, Y. Zhan, Y. Huang, L. Yang, X. Tu and S. Luo, "Removal of water-soluble acid dyes from water environment using a novel magnetic molecularly imprinted polymer", *J. Hazard. Mater.*, **2011**, 187, 274-282.
4. H. Bessbousse, T. Rhlalou, J. F. Verchère and L. Lebrun, "Removal of heavy metal ions from aqueous solutions by filtration with a novel complexing membrane containing poly(ethyleneimine) in a poly(vinyl alcohol) matrix", *J. Membr. Sci.*, **2008**, 307, 249-259.
5. G. Sen, S. Ghosh, U. Jha and S. Pal, "Hydrolyzed polyacrylamide grafted carboxymethyl starch (Hyd. CMS-g-PAM): An efficient flocculant for the treatment of textile industry wastewater", *Chem. Eng. J.*, **2011**, 171, 495-501.
6. D. Mantzavinos and E. Psillakis, "Enhancement of biodegradability of industrial wastewaters by chemical oxidation pre-treatment", *J. Chem. Technol. Biotechnol.*, **2004**, 79, 431-454.
7. B. Alyüz and S. Veli, "Kinetics and equilibrium studies for the removal of nickel and zinc from aqueous solutions by ion exchange resins", *J. Hazard. Mater.*, **2009**, 167, 482-488.
8. S. Barreca, S. Orecchio and A. Pace, "The effect of montmorillonite clay in alginate gel beads for polychlorinated biphenyl adsorption: Isothermal and kinetic studies", *Appl. Clay Sci.*, **2014**, 99, 220-228.
9. S. Cataldo, N. Muratore, S. Orecchio and A. Pettignano, "Enhancement of adsorption ability of calcium alginate gel beads towards Pd(II) ion. A kinetic and equilibrium study on hybrid laponite and montmorillonite-alginate gel beads", *Appl. Clay Sci.*, **2015**, 118, 162-170.
10. D. W. O'Connell, C. Birkinshaw and T. F. O'Dwyer, "Heavy metal adsorbents prepared from the modification of cellulose: A review", *Bioresour. Technol.*, **2008**, 99, 6709-6724.
11. P. Waranusantigul, P. Pokethitiyook, M. Kruatrachue and E. S. Upatham, "Kinetics of basic dye (methylene blue) biosorption by giant duckweed (*Spirodela polyrrhiza*)", *Environ. Pollut.*, **2003**, 125, 385-392.
12. L. G. da Silva, R. Ruggiero, P. M. Gontijo, R. B. Pinto, B. Royer, E. C. Lima, T. H. M. Fernandes and T. Calvete, "Adsorption of brilliant red 2BE dye from water solutions by a chemically modified sugarcane bagasse lignin", *Chem. Eng. J.*, **2011**, 168, 620-628.
13. A. D. Site, "Factors affecting sorption of organic compounds in natural sorbent/water systems and sorption coefficients for selected pollutants. A review", *J. Phys. Chem. Ref. Data*, **2001**, 30, 187-439.
14. M. Brigante, G. Zanini and M. Avena, "Effects of montmorillonite on the chemical degradation kinetics of metsulfuron methyl in aqueous media", *Appl. Clay Sci.*, **2103**, 80-81, 211-218.
15. H. Yan, W. Zhang, X. Kan, L. Dong, Z. Jiang, H. Li, H. Yang and R. Cheng, "Sorption of methylene blue by carboxymethyl cellulose and reuse process in a secondary sorption", *Colloids Surf. A Physicochem. Eng. Aspects*, **2011**, 380, 143-151.
16. I. Filpponen and D. S. Argyropoulos, "Determination of cellulose reactivity by using phosphorylation and quantitative <sup>31</sup>P NMR spectroscopy", *Ind. Eng. Chem. Res.*, **2008**, 47, 8906-

8910.

17. Y. Bao, J. Ma and N. Li, "Synthesis and swelling behaviors of sodium carboxymethyl cellulose-g-poly(AA-co-AM-co-AMPS)/MMT superabsorbent hydrogel", *Carbohydr. Polym.*, **2011**, *84*, 76-82.
18. M. Liu, Y. Deng, H. Zhan and X. Zhang, "Adsorption and desorption of copper (II) from solutions on new spherical cellulose adsorbent", *J. Appl. Polym. Sci.*, **2002**, *84*, 478-485.
19. E. K. Yetimoğlu, M. V. Kahraman, Ö. Ercan, Z. S. Akdemir and N. K. Apohan, "N-vinylpyrrolidone/acrylic acid/2-acrylamido-2-methylpropane sulfonic acid based hydrogels: Synthesis, characterization and their application in the removal of heavy metals", *React. Funct. Polym.*, **2007**, *67*, 451-460.
20. V. Bekiari, M. Sotiropoulou, G. Bokias and P. Lianos, "Use of poly(N,N-dimethylacrylamide-co-sodium acrylate) hydrogel to extract cationic dyes and metals from water", *Colloids Surf. A Physicochem. Eng. Aspects*, **2008**, *312*, 214-218.
21. H. Kaşgöz and A. Durmus, "Dye removal by a novel hydrogel-clay nanocomposite with enhanced swelling properties", *Polym. Adv. Technol.*, **2008**, *19*, 838-845.
22. Y. Zheng and A. Wang, "Evaluation of ammonium removal using a chitosan-g-poly (acrylic acid)/rectorite hydrogel composite", *J. Hazard. Mater.*, **2009**, *171*, 671-677.
23. X. Liu, X. Li, Z. Lu, X. Miao and Y. Feng, "Modified acrylic-based superabsorbents with hydrophobic monomers: Synthesis, characterization and swelling behaviors", *J. Polym. Res.*, **2011**, *18*, 897-905.
24. L. Sciascia, M. L. T. Liveri and M. Merli, "Kinetic and equilibrium studies for the adsorption of acid nucleic bases onto K10 montmorillonite", *Appl. Clay Sci.*, **2011**, *53*, 657-668.
25. S. S. Gupta and K. G. Bhattacharyya, "Adsorption of heavy metals on kaolinite and montmorillonite: A review", *Phys. Chem. Chem. Phys.*, **2012**, *14*, 6698-6723.
26. M. Wang and L. Wang, "Synthesis and characterization of carboxymethyl cellulose/organic montmorillonite nanocomposites and its adsorption behavior for Congo Red dye", *Water Sci. Eng.*, **2013**, *6*, 272-282.
27. P. Lertsutthiwong, D. Boonpuak, W. Pungrasmi and S. Powtongsook, "Immobilization of nitrite oxidizing bacteria using biopolymeric chitosan media", *J. Environ. Sci.*, **2013**, *25*, 262-267.
28. G. R. Mahdavinia, J. Hasanpour, Z. Rahmani, S. Karami and H. Etemadi, "Nanocomposite hydrogel from grafting of acrylamide onto HPMC using sodium montmorillonite nanoclay and removal of crystal violet dye", *Cellulose*, **2013**, *20*, 2591-2604.
29. P. Rojsitthisak, S. Khunthon, K. Noomun and S. Limpanart, "Response surface method to optimize the preparation of carboxymethyl cellulose from corn peel agricultural waste", *ScienceAsia*, **2017**, *43*, 8-14.
30. B. Y. Swamy and Y. S. Yun, "In vitro release of metformin from iron (III) cross-linked alginate-carboxymethyl cellulose hydrogel beads", *Int. J. Biol. Macromol.*, **2015**, *77*, 114-119.
31. L.-Y. Long, F.-F. Li, Y.-X. Weng and Y.-Z. Wang, "Effects of sodium montmorillonite on the preparation and properties of cellulose aerogels", *Polymers*, **2019**, *11*, E415.
32. Y. Bulut and H. Aydın, "A kinetics and thermodynamics study of methylene blue adsorption on wheat shells", *Desalination*, **2006**, *194*, 259-267.
33. H. A. Begum and M. K. B. Mahbub, "Effectiveness of carboxymethyl cellulose for the removal of methylene blue from aqueous solution", *Dhaka Univ. J. Sci.*, **2013**, *61*, 193-198.
34. H. Omidian, J. G. Rocca and K. Park, "Advances in superporous hydrogels", *J. Control. Release*, **2005**, *102*, 3-12.

35. G. Crini, "Kinetic and equilibrium studies on the removal of cationic dyes from aqueous solution by adsorption onto a cyclodextrin polymer", *Dyes Pigm.*, **2008**, 77, 415-426.
36. M. Dalaran, S. Emik, G. Güçlü, T. B. İyim and S. Özgümüş, "Study on a novel polyampholyte nanocomposite superabsorbent hydrogels: Synthesis, characterization and investigation of removal of indigo carmine from aqueous solution", *Desalination*, **2011**, 279, 170-182.
37. H. Kono, H. Hara, H. Hashimoto and Y. Shimizu, "Nonionic gelation agents prepared from hydroxypropyl guar gum", *Carbohydr. Polym.*, **2015**, 117, 636-643.
38. C. Chipot, R. Jaffe, B. Maigret, D. A. Pearlman and P. A. Kollman, "Benzene dimer: A good model for  $\pi$ - $\pi$  interactions in proteins? A comparison between the benzene and the toluene dimers in the gas phase and in an aqueous solution", *J. Am. Chem. Soc.*, **1996**, 118, 11217-11224.
39. T. W. Weber and R. K. Chakravorti, "Pore and solid diffusion models for fixed-bed adsorbers", *AIChE J.*, **1974**, 20, 228-238.
40. H. M. F. Freundlich, "Over the adsorption in solution", *J. Phys. Chem.*, **1906**, 57, 385-471.